Molecular BioSystems

Anticancer effects of novel resveratrol analogues on human ovarian cancer cells

Journal:	*Molecular BioSystems*
Manuscript ID	Draft
Article Type:	Paper
Date Submitted by the Author:	n/a
Complete List of Authors:	vergara, daniele; University of Salento, DISTEBA

Anticancer effects of novel resveratrol analogues on human ovarian cancer cells

Vergara Daniele[a,b,*], Stefania De Domenico[c], Tinelli Andrea[d,e], Stanca Eleonora[a,b], Loretta L. del Mercato[f], Anna Maria Giudetti[a], Simeone Pasquale[g], Nicola Guazzelli[h], Marco Lessi[h], Chiara Manzini[h], Angelo Santino[c], Bellina Fabio[h], Maffia Michele[a,b,**]

a) Department of Biological and Environmental Sciences and Technologies, University of Salento, via Monteroni, Lecce, Italy

b) Laboratory of Clinical Proteomic, ‘‘Giovanni Paolo II’’ Hospital, ASL-Lecce, Italy

c) Institute of Food Production Sciences, C.N.R. Unit of Lecce, via Monteroni, 73100 Lecce, Italy

d) Division of Experimental Endoscopic Surgery, Imaging, Technology and Minimally Invasive Therapy, Department of Obstetrics and Gynecology, Vito Fazzi Hospital, Piazza Muratore, Lecce , Italy

e) The International Translational Medicine and Biomodelling Research Group, Department of Applied Mathematics, Moscow Institute of Physics and Technology (State University), Moscow Region, Russia

f) CNR NANOTEC - Institute of Nanotechnology c/o Campus Ecotekne, Via Monteroni, 73100 Lecce, Italy

g) Department of Medicine and Aging Sciences, School of Medicine and Health Sciences, and Unit of Cytomorphology, Center of Aging Sciences and Translational Medicine (CeSI-MeT), University "G. d'Annunzio", Chieti-Pescara, Chieti, Italy.

h) Department of Chemistry and Industrial Chemistry, University of Pisa, Via Moruzzi 3, 56124 Pisa, Italy

***Correspondence to:** Daniele Vergara, Department of Biological and Environmental Sciences and Technologies, University of Salento, via Monteroni, Lecce, Italy, daniele.vergara@unisalento.it

****Correspondence to:** Michele Maffia, Department of Biological and Environmental Sciences and Technologies, University of Salento, via Monteroni, Lecce, Italy, michele.maffia@unisalento.it

Keywords: resveratrol, resveratrol analogues, ovarian cancer, epithelial mesenchymal transition

Abstract

Resveratrol, a naturally occurring phytoalexin, has long been known to have an important regulatory role of key functions in cell physiology. This multifunctional role of resveratrol is explained by its ability to interact with several targets of various cell pathways. In the recent past, synthetic chemical modifications have attempted to enhance the biological effects of resveratrol, including their anti-cancer properties. In this study, we investigated the molecular mechanisms of action of novel trans-restricted analogues of resveratrol in which the C–C double bond of the natural derivative has been replaced by diaryl substituted imidazole analogues.

In ovarian cancer models, results of *in vitro* screening revealed that analogues exhibited enhanced anti-proliferative properties compared with resveratrol. We found that resveratrol analogues also significantly inhibited Akt and MAPK signalling and reduced migration of IL-6 and EGF-treated cells. Finally, in ascites-derived cancer cells, we demonstrated that resveratrol analogues reduced the expression of epithelial mesenchymal transition (EMT) markers. Collectively, these findings indicated the enhanced anti-cancer properties of resveratrol analogues.

Introduction

The health benefits of dietary phytochemicals have been largely demonstrated. Evidence from epidemiological studies, animal and human trials has suggested a strong association between the consumption of plant nutrients and the prevention of several human diseases including cancer, neurological disorders, obesity and atherosclerotic cardiovascular diseases.[1-3] The beneficial effects of dietary compounds have been attributed to the presence of several classes of molecules classified as carotenoids, phenolics, alkaloids, nitrogen-containing compounds, and organosulfur compounds.[4] Among these, phenolics are molecules possessing at least one aromatic ring with one or more hydroxyl groups into the phenyl ring with the potential to interact with cellular proteins. For this property, this class of metabolites is the subject of an extensive medical research for its ability to act as antioxidants and as anticancer agents via regulation of signal transduction pathways. Resveratrol (3,5,4'-trans-trihydroxystilbene) is a naturally occurring phenolic compound that is found in a variety of food sources, including wine, soy, peanuts, and peanut products.[5,6] Since 1997 when Jang and colleagues reported the ability of resveratrol to inhibit carcinogenesis at multiple stages,[7] this molecule has gained particularly attention due to its inhibition of cellular events associated with tumor initiation, promotion and progression.[8] The cellular mechanisms contributing to the beneficial effects of resveratrol include the inactivation of multiple cellular pathways that regulate cell survival or apoptosis. Mechanisms include the downregulation of protein kinases including nuclear factor (NF)-κB, Wnt/β-catenin, protein kinase B (Akt), and mitogen-activated protein kinases (MAPK).[9-11] Parametric analysis of gene set enrichment (PAGE) indicated that resveratrol caused a significant alteration in 127 pathways including those involved in the regulation of cellular metabolism and Stat3 signalling.[8]

These observations clearly reported the potential application of resveratrol in a clinical setting. However, results obtained *in vitro* were only partially reported *in vivo*.[12] A major challenge that limits the potential application of resveratrol in human studies is represented by its poor bioavailability and the discrepancy between the concentrations used in cellular studies and those applied *in vivo*. Therefore, studies are ongoing to enhance the bioavailability of resveratrol by combinations with agents that can increase the *in vivo* metabolism, nanoparticle-mediated delivery, and the development of resveratrol based analogues.[13,14]

In this paper, we designed new analogues of resveratrol in which their stereochemically defined "trans" carbon-carbon double bond(s) has been locked into (hetero)cyclic moieties.[15] This strategic choice is founded on the fact that in the conversion of resveratrol into biologically inactive metabolites *in vivo*, the chemical liability of these double bonds, which suffer from trans-to-cis stereoisomerization and reduction to saturated carbon-carbon bonds, is involved.[16,17] In detail, we

plan to replace the trans-configured carbon-carbon double bond(s) of resveratrol scaffolds with five-membered heterocycles. In order to keep the trans geometry of the leading phytochemicals, the aromatic substituents were attached to the heterocyclic core in a 1,3-fashion.

The anti-tumorigenic activity of all these compounds was evaluated in the ovarian cancer cell line SKOV-3 and primary cancer cells isolated from the ascites of patients with metastatic ovarian cancer, and compared to that of resveratol. The abilities of these new derivates to reduce cell adhesion, cell migration and their potential synergy with chemotherapeutic drugs were also tested. The tested derivates were shown to possess greater anti-tumorigenic properties than resveratrol. This lays the foundation for future exploration in preclinical models.

Experimental

Compounds and reagents

Collagen type IV, MTT (3-[4,5-dimethylthiazol-2-yl]-2,5-diphenyl tetrazolium bromide), and resveratrol were purchased from Sigma-Aldrich (St Louis, MO). Resveratrol was dissolved in dimethyl sulfoxide (DMSO) and immediately used. Epidermal growth factor (EGF), and Interleukin-6 (IL-6) were from Prospec. Paclitaxel (PTX) was purchased from Tocris (Bristol, UK). The pan-caspase inhibitor Z-VAD-FMK was form Abcam (Cambridge, UK). The following reagents were obtained from GE Healthcare (Little Chalfont, UK): Hybond ECL membrane and ECL western blotting detection reagents. Fibronectin was from BD Biosciences (San Jose, CA). Primary antibodies were listed in (Supplementary Table 1). Secondary antibodies (HRP-conjugated) were all from Santa Cruz Biotechnology (Dallas, Texas). Cell culture media and reagents were purchased from EuroClone (Milano, Italy). All other reagents were from standard commercial sources and were of the highest grade available.

The synthesis of resveratrol analogues was performed as previously described.[18] Briefly, 1,4-diaryl-1*H*-imidazoles Res_04, Res_08, Res_10, Res_15, Res_16, and Res_18, were prepared by a palladium-catalyzed Suzuki cross coupling reaction involving commercially available arylboronic acids and 4-bromo-1*H*-imidazole, followed by a copper-catalyzed Buchwald *N*-arylation of the resulting 4-aryl-1*H*-imidazoles with the required aryl bromides. On the contrary, 2,5-diaryl-1-methyl-1*H*-imidazole Res_09, Res_11, Res_12, Res_13, Res_14, and Res_19 were regioselectively obtained by a palladium and copper promoted sequential C5/C2 double arylation of 1-methyl-1*H*-imidazole with the required aryl bromides. All the compounds were isolated by flash chromatography on silica gel, and gave satisfactory mps, ^{1}H-NMR, ^{13}C-NMR, elemental analyses,

and EIMS data. GLC analyses showed that their chemical purity was higher than 97%. The chemical structure of analogues is shown in Supplementary Fig. 1. Analogues were all dissolved in in DMSO.

Cell culture

SKOV-3 human ovarian cancer cell line was grown in high-glucose Dulbecco's modified Eagle's medium (DMEM) supplemented with 10% fetal bovine serum (FBS), 2-mM L-glutamine, 100 U mL^{-1} penicillin, 100 μg mL^{-1} streptomycin, in a humidified atmosphere of 5% CO_2 at 37 °C.

Normal Human Dermal Fibroblasts (NHDF) were kindly provided by dr. Tiziana Cocco and dr. Antonio Gaballo and maintained under standard culture conditions (complete DMEM, 5% CO_2 at 37 °C). MDA-231 cells were maintained under standard culture conditions (complete DMEM, 5% CO_2 at 37 °C).

Ascites were collected from chemotherapy-naïve ovarian cancer patients (n=3) diagnosed with serous adenocarcinoma and presented as stage III (FIGO classification) at the time of clinical intervention, as previously described.[19] All patients provided written informed consent.

Cell viability assay

Cells were plated at 5 x 10^3 / well in a 96-well plate and allowed to adhere to the plate overnight under the growth conditions described above. For determining cell viability, the MTT assay was used. After treatment, the culture medium was aspirated and 100 μl of RPMI-phenol free medium containing 10 μl of MTT stock solution, 5 mg mL^{-1} in phosphate-buffered saline (PBS) solution, was added to each well. After one hour of incubation, the MTT solution was removed and 100 μl of DMSO were added to dissolve MTT-formazan crystals. Absorbance of the converted dye was measured at a wavelength of 570 nm using an iMark microplate reader (BIORAD). The relative cell viability was expressed as a percentage of the untreated control group. The concentration of drug required to inhibit cell proliferation by 50% (IC50) was calculated using the Microsoft Excel software. Data were exported and analyzed using an Excel sheet and IC50 values were calculated by linear interpolation. IC values are expressed as mean ± standard deviation from at least ten independent experiments.

Cell adhesion assay

Cells were treated with resveratrol or analogues, maintained in suspension for 1 hour, and seeded onto 96-well plates coated with fibronectin (10 μg mL^{-1}) or collagen type IV (10 μg mL^{-1}) for 1 h at 37 °C, at a density of 1×10^5 cells/well. Bovine serum albumin (BSA) coating was used as negative

control. Briefly, non-adherent cells were removed by washing with PBS. Attached cells were fixed with 70% methanol for 10 minutes. Cells were stained with 0.02% crystal violet in 0.2% ethanol solution. Incorporated dye was dissolved in 10% acetic acid, and the absorbance was measured at 560 nm. Each experiment was done in triplicate.

Scratch wound assay

Cells were cultured 24-well plate until confluence and then wounded using a 200 μL pipette tip in the middle of well. Three wounds were made for each sample, and migration distance was photographed and measured at zero time and after 24 h under an Olympus IX-51 microscope. The percentage (%) of open wound area was determined and the change in open wound area (%) at 24-hour against zero time was calculated using the GraphPad PRISM software version 4.0.

Western blot analysis

Whole proteins were extracted in RIPA buffer (Cell Signaling, Danvers, MA) and quantified by the Bradford protein assay (BIORAD, Hercules, CA). Samples were separated by 12% SDS–PAGE and transferred to Hybond ECL nitrocellulose membranes (GE Healthcare, Little Chalfont, UK). The membranes were blocked with Blotto A (Santa Cruz, Dallas, Texas) at room temperature for 1 h, and incubated with the appropriate primary antibodies (see Supplementary Table 1) for 2 h at room temperature, as previously performed.[20] After two washes with a solution of TBS containing 0.1% (v/v) tween 20 for 10 min, the membranes were incubated with secondary antibody HRP-conjugated for 2 h at room temperature (standard dilution 1:2000). Blots were then developed using the Amersham ECL western blotting detection system (GE Healthcare, Little Chalfont, UK). Densitometric quantitation of at least three indipendent replicates was done using ImageJ software.

Nucleic acid extraction, cDNA synthesis and qRT-PCR analysis

Total RNA was isolated from SKOV-3 cells using the Illustra triplePrep kit (GE Healthcare, Little Chalfont, UK). First-strand cDNA was synthesized using 1 μg of total RNA, oligo(dT)18 and SuperScript III reverse transcriptase (Invitrogen, San Diego, CA) according to the manufacturer's protocol. The transcription profiles of *CDH2*, *Slug, Vimentin, Zeb1, Zeb2, Sirt1, NRF1, TFAM, PPARGC1A* genes after different treatment were analysed by using real time quantitative reverse transcription-PCR (qRT-PCR), which was performed in a 7500 Real-Time PCR System (Applied Biosystem, Warrington, UK). For the amplification reaction, a SYBR Green assay with iTaq Universal SYBR Green supermix (Bio-Rad, Hercules, CA) was performed in a reaction volume of 25 μl. Expression levels of each mRNA were normalized to those of *Rplp0* mRNA. Primers and

respective concentrations used for qRT-PCR are listed in Supplementary Table 2. The following amplification conditions were used: an initial denaturation step at 95 °C for 2 min, followed by 40 cycles of 15 sec at 95 °C and 40 sec at 60 °C. Three replicates were performed for each experiment in addition to a no-template control included for each primer pair. Specificity of the PCR amplification was confirmed by dissociation curve analyses and the relative quantification of gene expression was established using the comparative $2^{-\Delta\Delta CT}$ method.

Statistical analysis

Data were expressed as mean ± SD. Statistical analyses was determined by unpaired Student's t-test to compare between two groups and One-way ANOVA to compare three groups, analyzed using GraphPad PRISM software version 4.0. In all comparisons, $p<0.05$ was considered as statistically significant.

Results

The anti-proliferative effect of twelve analogues of resveratrol was evaluated in the human ovarian cancer cell line SKOV-3 using the MTT proliferation assay. Cells were treated with *trans*-resveratrol, used as a reference compound, and its analogues at the concentrations of 100 μM, 50 μM, and 25 μM, for 24 and 72 h (Fig. 1). Results show that all the analogues tested inhibited cell proliferation in a dose- and time-dependent manner (Fig. 1a). As shown in table 1, the IC50 (drug concentration required to reduce of 50% cell viability) values calculated for resveratrol and analogues demonstrated that resveratrol derivates exhibited a higher anti-proliferative activity compared to resveratrol treatment alone. In detail, at 100 μM and after 24 h of exposure, analogues 4, 12, 13, 15, 16, and 19 produced the most pronounced effect with 100 % suppression of cellular growth (Fig. 1a). In contrast, cell viability of NHDF cells was not affected after resveratrol analogues treatment (Supplementary Figure 2). These data showed that analogues specifically reduced the growth of tumor cells but not normal cells *in vitro*.

Biological effects of analogues on cancer cells were first assessed by investigating the expression of proteins related to the regulation of cell viability and proliferation, cytoskeletal rearrangement, and cell-cell adhesion. Changes in cell morphology (loss of front–back polarity and gain of organized compact cell island) were also evaluated microscopically. For this screening, we selected analogues 4, 12, 13, 15, 16, and 19 that exhibited the greater anti-proliferative effect after 24 h of treatment.

We previously demonstrated the reduced phosphorylation of Akt/Gsk, and Erk as a mechanism of cell growth inhibition mediated by resveratrol,[21] leading to the hypothesis that these proteins may

also be a candidate targets for analogues in ovarian cancer models. Therefore, in the present study we treated SKOV-3 cells with resveratrol and analogues at 50 μM for 1 h, and compared the expression levels of selected proteins by western blotting. As shown in Fig. 1b, the phosphorylation levels of Akt, Gsk, Erk, and cofilin (Cof) were significantly reduced in SKOV-3 after treatment. We also demonstrated the reduced protein expression of N-cadherin, cyclin D1, β-catenin, and Bcl2 in SKOV-3 cells treated with analogues (Fig. 1b and Supplementary Figure 3). Collectively, these results imply that analogues-mediated anti-proliferative effects are mediated through the down-regulation of survival and proliferation protein kinase signaling pathways such as Akt and Erk.

In addition to these effects on cell proliferation, analogues demonstrated anti-tumor activities towards other cellular processes, including cell adhesion on extracellular matrix components (ECM) and cell migration. To demonstrate this, we tested the adhesion of SKOV-3 cells on cell culture plastic wells coated with two different ECM components, fibronectin and collagen IV, for 30 min and 4 h. As a control, an equal number of cells was added to uncoated wells or wells coated with BSA. Figure 2 showed the reduced adhesion to matrix proteins in SKOV-3 cells treated with resveratrol or analogues after 30 min and 4 h. As shown, there was a significant decrease of cell adhesion after treatment with analogues 4, 10, 12, 13, 14, 15, 16, and 19.

In vitro scratch wound healing assays showed that the migration of SKOV-3 cells was significantly inhibited in the presence of analogues (Fig. 3a, b). The rate of wound closure was different depending on analogues exposure, but significantly reduced compared to EGF- and IL-6-exposed cells. Fig. 3d shows representative images of a scraping assay after resveratrol and analogues treatment. The upper panels show the cell position at 0 hours, while the other panels the gap closure after EGF and IL-6 treatment alone or in co-stimulation with resveratrol and selected analogues. Among the analogues tested, Res_4 showed the most pronounced effects on cell motility. We explored the molecular mechanisms behind Res_4 action, by examining the possible modulation of EGF downstream signalling pathways. To demonstrate this, we treated cancer cells with EGF alone or in co-stimulation with Res_4 at two different time points, and examined changes in the phosphorylation status of Erk (pErk). As shown in Fig 3c, Res_4 treatment caused a significant reduction of pErk levels as compared to EGF and EGF plus resveratrol treated cells. These results were consistent with the functional effects observed after wound assay.

Suppression of cell migration, modulation of cytoskeletal components (i.e. cofilin), and down-regulation of mesenchymal markers (i.e. N-cadherin) are reminiscent of a re-differentiation towards an epithelial phenotype, through the activation of a mesenchymal-epithelial transition (MET) program, which is the reverse process of the epithelial mesenchymal transition (EMT).[22] We then examined whether analogues treatment would mediate a phenotypic and functional transition to

MET. To demonstrate this, we performed a RT-qPCR analysis of EMT markers including key EMT-activating transcription factors, Zeb1, Zeb2, and Slug, to assess transcriptomic changes induced after resveratrol and analogues treatment (Fig. 4). Among the analogues tested, we selected Res_15 for its enhanced anti-proliferative properties observed in the screening analysis. As shown, all five genes tested were down-regulated significantly after Res_15 treatment at 25 μM for 24 h. On the contrary, after Res treatment at 100 μM for 24 h, only Vimentin expression level was reduced whereas Zeb2 and Slug increased significantly their expression (Fig. 4a). Hence, Res_15 treatment affected better than resveratrol the expression of EMT markers in SKOV-3 cells. After demonstrating the reduced expression levels of these genes after analogues treatment, we determined phenotypic modifications induced in SKOV-3 after treatment with resveratrol or analogues to observe a potential reversion to an epithelial status (Fig. 4b). The morphological appearance of treated SKOV-3 cells is illustrated in Fig. 4b. Despite the changes in EMT markers, the protein levels of the epithelial marker E-cadherin remained undetectable by western blotting (Fig. 1b), with no significant reversal of cell morphology (Fig. 4b). Similar results were obtained by treating the mesenchymal breast cancer model MDA-231 with analogues for 72 h and observing cell modifications by phase-contrast morphology (data not shown), leading to the conclusion that analogues reduced the expression of EMT markers and signalling EMT-related pathways without a complete molecular and phenotypic reversion into tight epithelial clusters.

These enhanced anti-cancer properties prompted us to investigate the action of analogues respect to classical resveratrol targets. Previous studies described the ability of resveratrol to activate SIRT1 and transcriptional factors that regulate mitochondrial biogenesis. We then investigated whether Res_15 is able to activate these markers by RT-qPCR. As shown, SIRT1 and PGC1α mRNA levels were both higher after resveratrol and Res_15 treatment, but significantly lower in Res_15 treated cells (Supplementary Figure 4). This suggests that the chemical structure of resveratrol is functionally important for driving the activation of these markers.

The effects of analogues were also tested using ex-vivo models. Three primary cell lines were obtained form the ascitic fluid of from late-stage (III) ovarian serous adenocarcinoma cancer patients. These cells were cultured *in vitro* as monolayer or forced to growth in suspension using poly-HEMA coated-plates. We tested the anti-proliferative effect of analogues on these cell lines, these results are shown in Table 2. Reduced cell proliferation was demonstrated in ascitic cells compared with resveratrol treated cells. The most significant effects were obtained with Res_15, which was further studied for its ability to reduce growth is suspension and to reduce the expression of EMT markers (Fig. 5). Primary ovarian cancer cells were maintained in suspension using poly-HEMA, which prevents cell attachment to the substratum and treated with resveratrol and Res_15

(Fig. 5a). As shown, in primary tumor cells and tumor cell lines, the percentage of trypan blue positive cells significantly increased after resveratrol and Res_15 exposure (Fig. 5a and b). Exposure of primary tumor cells to pan-caspase inhibitor Z-VAD-FMK, prevented resveratrol and Res_15 cell death suggesting that apoptosis is involved in the mechanism of cell death induced after resveratrol and its analogue exposure (Fig. 5a). The molecular mechanism underlying Res_15 effects were investigated with a particular interest towards the regulation of EMT markers, cell cycle and apoptosis proteins. Res_15 reduced N-cadherin, Vimentin, Slug, Zeb1, Cyclin D1, Bcl2 protein expression, and increased the expression of E-cadherin (Fig. 5c).

EGF and IL-6 reduced the anti-cancer effect of the chemotherapeutic agent Paclitaxel (PTX) on tumor cells (Table 3). To verify if Res_15 analogue can interfere with this mechanism, we treated primary cells with PTX alone or in combination with EGF, IL-6, resveratrol and Res_15. As shown in Table 3, EGF and IL-6 in combination with PTX reduced the responsiveness to drug treatment, while resveratrol and Res_15 restore chemotherapy response. Both molecules act by targeting the EGF-induced pErk activation, as shown in Fig. 5d.

Discussion

We previously demonstrated the anticancer properties of trans-restricted analogues of resveratrol *in vitro* against 60 human tumor cell lines (National Cancer Institute-60 panel).[18] Analogues displayed significant anti-proliferative potential across the NCI 60 panel. It remains to be determined the relationships among these analogues and resveratrol targets. In the present study, we provided further insights about the molecular targets of tested compounds using *in vitro* and *ex vivo* ovarian cancer cell models that we previously characterised for the resveratrol-mediated tumor suppressing activities.

Our *in vitro* studies confirmed that resveratrol analogues reduced proliferation, cell-adhesion on ECM components, EGF- and IL-6-induced cell migration, EGF- and IL-6-induced chemoresistance, and anchorage independent growth of ovarian cancer cells. Resveratrol analogues affected cell proliferation in a dose and time dependent manner with an IC50 at 24 h and 72 h lower than resveratrol, without affecting the proliferation of normal cells. Among the analogues, Res_4, Res_12, Res_13, Res_15, Res_16, and Res_19 showed the lower IC50 at 24 h and were further evaluated by western blotting against some selected protein targets. These analogues belong to two main groups: Res_4, Res_15, Res_16 are 1,5-diaryl substituted imidazoles, while Res_12, Res_13, and Res_19 are 2,5-diaryl substituted 1-methylimidazoles. Our previous report suggested that the anti-proliferative effect of resveratrol was mediated through affecting Akt, Gsk, and Erk pathways.[21] For this reason, we sought to investigate whether the same mechanism occurred also in

SKOV-3 cells treated with analogues. Our proposed model for analogues-induced antiproliferative effects in SKOV-3 is *via* the inhibition of Akt, Gsk, and Erk phosphorylation, and the reduced protein expression of cyclin D1, Bcl2 and β-catenin. Consistent with the observed morphological changes, a modification of cofilin phosphorylation was observed after treatment. Analogues also decreased the expression of N-cadherin but did not restore the expression of the epithelial marker E-cadherin. N-cadherin mRNA down-regulation was confirmed by RT-qPCR, together with a significant effects of other EMT markers. This response was not observed after resveratrol treatment indicating a better activity of analogues against EMT markers.

Overall, these data indicate the ability of analogues to be efficacious against several cellular targets, including EMT transcriptional regulators, a biological property that already characterises resveratrol and explains its multi-functional role in cell physiology. Importantly, analogues demonstrated a significant therapeutic potential at concentrations lower than those of resveratrol making these molecules closer to a possible clinical application.

One of the physiological consequences of resveratrol treatment is the activation of energy sensing bioenergetics markers and pathways. We investigated the extent of analogues effects on these resveratrol targets. *SIRT1* and *PPARGC1A* are typically activated after resveratrol treatment. The present data demonstrate that the activation at mRNA level of SIRT1 and PGC1α were lower in Res_15 treated cells compared to resveratrol treatment. This results can be explained by considering i) the lower concentration of Res_15 that we used to stimulate cells; ii) a close structure-activity relationship that is important to activate these pathways. This hypothesis is also supported by other studies that described the structure-activity relationships of various polyphenols including resveratrol.[23]

Despite highly similar in their chemical structure, analogues demonstrate different biological properties. As shown in Fig. 1 and Supplementary Fig. 3, all six tested analogues exerted their effects by targeting cyclin D1, pErk (thr202/tyr204), pGsk (ser9), and pAkt (ser473). Three analogues (Res_15, Res_16, and Res_19) emerged in this screening because they showed greater effectiveness against some of the investigated targets (Supplementary Fig. 3), N-cadherin, β-catenin, and Bcl2. These results provide a link between the chemical structure of analogues and their biological properties. This is also confirmed in the adhesion and wound experiments where analogues Res_4 showed greater efficacy compared to the other compounds.

Of various resveratrol analogues tested, Res_15 showed the greater anti-proliferative effect, and was further assayed for its anti-cancer properties against patients-derived *ex-vivo* cultures isolated from ascetic fluids. Compared to SKOV-3, which are molecularly characterised by the expression of mesenchymal markers, ascites-derived cells exhibited an intermediate EMT phenotype as

evidenced by the simultaneous co-expression of epithelial and mesenchymal proteins. This is a more informative experimental system to detect changes in protein expression on a larger panel of EMT markers after analogues treatment. Overall, results confirmed the greater anti-cancer properties of Res_15 compared to resveratrol. Major mechanisms of action appear to involve the down-regulation of mesenchymal proteins with a significant up-regulation of the epithelial marker E-cadherin, suggesting that the intermediate mesenchymal phenotype can be partially reversed after treatment. This observation highlights the ability of resveratrol to target EMT/MET markers, but marks a difference compared to the experiments performed on SKOV-3. In this cell model, resveratrol and analogues were unable to restore E-cadherin expression. This means, that the mechanisms behind the repression of E-cadherin expression in SKOV-3 do not respond to resveratrol and analogues treatment. It remains unclear whether this was due to the incomplete repression of EMT transcriptional factors by Res_15 or due to the presence of an epigenetic mechanism of control.

The MAPK pathway is closely associated with chemoresistance. The activation of this pathway is one of the mechanisms at the basis of PTX resistance.[21] As demonstrated, analogues exhibited Erk inhibition. For this reason we tested the possibility to use analogues for overcoming EGF- and IL-6 mediated resistance of cancer cells after PTX treatment. Here, we demonstrated the antagonizing effects of Res_15 on Erk phosphorylation mediated by EGF and IL-6 in combination with PTX in primary cells.

Taken together, the current study highlights the potential of imidazole based resveratrol analogues, and indicates that Res_15 can be considered as a potential scaffold for the development of novel analogues with greater therapeutic potential against ovarian cancer.

Acknowledgments

We gratefully acknowledge funding from the Apulia Regional Cluster project “SISTEMA” project code T7WGSJ3. We thank dr. Antonio Danieli for his technical assistance.

Author Contributions

D.V. designed experiments. M.F. obtained funding, and supervised the study. D.V., S.D.D., and S.E. performed the experiments. A.M.G., S.P., L.D.M., and A.S. analysed data. A.T. was involved in sample collection. N.G., M.L., C.M., and B.F performed the design and synthesis of analogues. D.V. wrote the paper. All authors read and approved the final manuscript.

Conflict of interest

Authors declare that there is no conflict of interest.

References

1. Del Rio D, Rodriguez-Mateos A, Spencer JP, Tognolini M, Borges G, Crozier A. 2013. Dietary (Poly)phenolics in Human Health: Structures, Bioavailability, and Evidence of Protective Effects Against Chronic Diseases. Antioxid Redox Signal 18:1818-1892.
2. McCullough ML, Peterson JJ, Patel R, Jacques PF, Shah R, Dwyer JT. 2012. Flavonoid intake and cardiovascular disease mortality in a prospective cohort of US adults. Am J Clin Nutr 95:454-464.
3. Slavin JL. Lloyd B. 2012. Health benefits of fruits and vegetables. Adv Nutr 3:506-516.
4. Liu RH. Potential synergy of phytochemicals in cancer prevention: mechanism of action. 2004. J Nutr 134:3479S-3485S.
5. Baur JA, Sinclair DA. 2006. Therapeutic potential of resveratrol: the in vivo evidence. Nat Rev Drug Discov 5:493-506.
6. Burns J, Yokota T, Ashihara H, Lean ME, Crozier A. 2002. Plant foods and herbal sources of resveratrol. J Agric Food Chem 50:3337-3340.
7. Jang M, Cai L, Udeani GO, Slowing KV, Thomas CF, Beecher CW, Fong HH, Farnsworth NR, Kinghorn AD, Mehta RG, Moon RC, Pezzuto JM. 1997. Cancer chemopreventive activity of resveratrol, a natural product derived from grapes. Science 275:218-220.
8. Baur JA, Pearson KJ, Price NL, Jamieson HA, Lerin C, Kalra A, Prabhu VV, Allard JS, Lopez-Lluch G, Lewis K, Pistell PJ, Poosala S, Becker KG, Boss O, Gwinn D, Wang M, Ramaswamy S, Fishbein KW, Spencer RG, Lakatta EG, Le Couteur D, Shaw RJ, Navas P, Puigserver P, Ingram DK, de Cabo R, Sinclair DA. 2006. Resveratrol improves health and survival of mice on a high-calorie diet. Nature. 444:337-342.
9. Vergara D, Simeone P, Toraldo D, Del Boccio P, Vergaro V, Leporatti S, Pieragostino D, Tinelli A, De Domenico S, Alberti S, Urbani A, Salzet M, Santino A, Maffia M. 2012. Resveratrol downregulates Akt/GSK and ERK signalling pathways in OVCAR-3 ovarian cancer cells. Mol Biosyst 8:1078-1087.
10. Vergara D, Valente CM, Tinelli A, Siciliano C, Lorusso V, Acierno R, Giovinazzo G, Santino A, Storelli C, Maffia M. 2011. Resveratrol inhibits the epidermal growth factor-induced epithelial mesenchymal transition in MCF-7 cells. Cancer Lett 310:1-8.
11. Kundu JK, Surh YJ. 2008. Cancer chemopreventive and therapeutic potential of resveratrol: mechanistic perspectives. Cancer Lett 269:243-261.
12. Subramanian L, Youssef S, Bhattacharya S, Kenealey J, Polans AS, van Ginkel PR. 2010. Resveratrol: challenges in translation to the clinic--a critical discussion. Clin Cancer Res 16:5942-5948.
13. Neves AR, Lucio M, Lima JL, Reis S. 2012. Resveratrol in medicinal chemistry: a critical review of its pharmacokinetics, drug-delivery, and membrane interactions. Curr Med Chem 19:1663-1681.
14. Szekeres T, Fritzer-Szekeres M, Saiko P, Jäger W. 2010. Resveratrol and resveratrol analogues--structure-activity relationship. Pharm Res 27:1042-1048.
15. Mayhoub AS, Marler L, Kondratyuk TP, Park EJ, Pezzuto JM, Cushman M. Optimizing thiadiazole analogues of resveratrol versus three chemopreventive targets. 2012. Bioorg Med Chem 20:510-520.
16. Walle T. 2011. Bioavailability of resveratrol. Ann N Y Acad Sci 1215:9-15.
17. Stivala LA, Savio M, Carafoli F, Perucca P, Bianchi L, Maga G, Forti L, Pagnoni UM, Albini A, Prosperi E, Vannini V. 2001. Specific structural determinants are responsible for the antioxidant activity and the cell cycle effects of resveratrol. J Biol Chem 276:22586-22594.
18. Bellina F, Guazzelli N, Lessi M, Manzini C. 2015. Imidazole analogues of resveratrol: synthesis and cancer cell growth evaluation. Tetrahedron 71:2298-2305.

19. Vergara D, Simeone P, Bettini S, Tinelli A, Valli L, Storelli C, Leo S, Santino A, Maffia M. 2014. Antitumor activity of the dietary diterpene carnosol against a panel of human cancer cell lines. Food Funct 5:1261-1269.
20. Vergara D, Simeone P, Latorre D, Cascione F, Leporatti S, Trerotola M, Giudetti AM, Capobianco L, Lunetti P, Rizzello A, Rinaldi R, Alberti S, Maffia M. 2015. Proteomics analysis of E-cadherin knockdown in epithelial breast cancer cells. J Biotechnol 202:3-11.
21. Vergara D, Bellomo C, Zhang X, Vergaro V, Tinelli A, Lorusso V, Rinaldi R, Lvov YM, Leporatti S, Maffia M. Lapatinib/Paclitaxel polyelectrolyte nanocapsules for overcoming multidrug resistance in ovarian cancer. 2012 Nanomedicine 8:891-899.
22. Vergara D, Merlot B, Lucot JP, Collinet P, Vinatier D, Fournier I, Salzet M. 2010. Epithelial-mesenchymal transition in ovarian cancer. Cancer Lett 291:59-66.
23. Takizawa Y, Nakata R, Fukuhara K, Yamashita H, Kubodera H, Inoue H. 2015 The 4'-hydroxyl group of resveratrol is functionally important for direct activation of PPARα. PLoS One 10(3):e0120865.

Figure Legends

Figure 1. Resveratrol analogues affect cancer cell viability. a) Skov-3 cells were treated with resveratrol or analogues at the indicated concentrations for 24 h or 72 h. Compounds were dissolved in DMSO and diluted to the desired concentration in DMEM medium. Control cells contained the vehicle only. Cell viability was calculated as described in Materials and Methods. Data shown represent the mean ± SD of three independent experiments and values were taken from at least six wells from each experiment. (b) E-cadherin, N-cadherin, Cyclin D1, Bcl-2, β-catenin, COF, pCOF, ERK, pERK, GSK, pGSK, Akt, pAkt protein expression was analyzed by western blot in SKOV-3 cells after treatment of 1 h with resveratrol or its analogues at the concentration of 50 μM; α-tubulin was used as loading control.

Figure 2. Resveratrol analogues reduce cancer cell adhesion on fibronectin- and collagen-coated plates. SKOV-3 were pre-treated with resveratrol or analogues for 1 h at the concentration of 50 μM and then seeded onto 10 μg mL^{-1} fibronectin-coated 96-well plates (a) or 10 μg mL^{-1} collagen-coated 96-well plates (b). Data are mean ± SD of three independent experiments expressed as percentage comparing with the control without treatment. Asterisks indicate a significant difference compared to resveratrol-treated samples. Student's t-test * $p<0.05$; ** $p<0.01$; *** $p<0.001$;

Figure 3. Resveratrol analogues reduce the IL-6- and EGF-induced migration of cancer cells. a and b) Histograms show quantitative analysis of the percentage of gap reduction in SKOV-3 cancer cells after treatment with EGF 100 ng mL^{-1} or IL-6 20 ng mL^{-1} alone or in combination with resveratrol analogues. Vertical bars indicate the percentage (mean ± SD of three independent experiments) of wound closure at 24 h compared to the wound distance at time 0 in the control group. Asterisks indicate a significant difference compared to resveratrol plus EGF and IL-6 treated samples. Student's t-test ** $p<0.01$; *** $p<0.001$. c) Representative immunoblots of Erk1/2 phosphorylation in SKOV-3 cells treated for 15 minutes or 4 h with EGF, resveratrol and EGF, Res_04 and EGF. Asterisks indicate a significant difference compared to resveratrol-treated samples. d) Representative images of wound healing assay showing the reduced migration of SKOV-3 treated cells after EGF and IL-6 stimulation.

Figure 4. a) Effects of Resveratrol and Res_15 treatment on gene expression in SKOV-3 cells. qPCR analysing the expression of EMT targets in SKOv-3 cells treated for 24 h with Res and Res_15 at the concentration of 100 uM and 25 uM, respectively. Data are represented as mean ± SD of three independent experiments. The only asterisks indicate a significant difference compared to control, whereas asterisks above a line represent a significant difference between resveratrol and Res_15 treated samples. One-way ANOVA analysis * $p<0.05$; ** $p<0.01$; *** $p<0.001$. b) Representative microscopic images of SKOV-3 cells treated with resveratrol or its analogues Res_04, Res_12, Res_13, Res_15, Res_16, Res_19 at the concentration of 25 μM and observed after 24 h of treatment (10x magnification).

Figure 5. Multiple anti-cancer effects of resveratrol analogues on primary ovarian cancer cells. a) A representative phase contrast microscope image of ascites-derived cancer cells maintained in suspension using poly-Hema coated dishes (magnification 10x, scale bar 100 μM) and treated with resveratrol (II), or Res_15 (III). Control cells were treated with vehicle (I). Ascites-derived human tumor cells were maintained in suspension using poly-Hema coated dishes and with or without pre-treatment of 50 mM ZVAD-fmk for 30 min prior to exposure to resveratrol or Res_15 for 72 h. The histograms show the percentage of positive cells for trypan blue staining. b) Human tumor cells were maintained in suspension using poly-Hema coated dishes and treated with resveratrol or Res_15 for 72 h. The histograms show the percentage of positive cells for trypan blue staining. Data

are the mean ± S.D of at least three independent experiments. Asterisks indicate a significant difference compared to res-treated samples. c) E-cadherin, N-cadherin, Vimentin, Slug, Zeb1, Cyclin D1, and Bcl2 protein expression was analyzed by western blot in ascites-derived ovarian cancer cells after treatment of 24 h with resveratrol or Res_15 at their IC50; α-tubulin was used as loading control. Densitometric quantification of three independent experiments (mean ± SD) was performed with ImageJ. Asterisks indicate a significant difference compared to resveratrol-treated samples. Student's t-test * $p<0.05$; ** $p<0.01$; *** $p<0.001$. d) Erk 1/2, and pErk (thr202/tyr204) protein expression were analysed by western blotting in ascites-derived cancer cells (OvCa1) treated with PTX (6 nM), EGF (100 ng mL^{-1}), Res (40 μM), and Res_15 (10 μM) after 4h of stimulation, as described. Asterisks indicate a significant difference compared to resveratrol-treated samples.

Table 1. IC50 values were calculated by performing dose-response experiments with resveratrol and analogues in SKOV-3 cells.

Compound	Chemical name	IC_{50}[a] 24h (μM)	IC_{50} 72h (μM)
Res	3,5,4'-trans-trihydroxystilbene	> 100	47.98 ± 1.31
Res_04	4-(4-methoxyphenyl)-1-(3,4,5-trimethoxyphenyl)-1*H*-imidazole	52.74 ± 1.4	24.29 ± 0.93
Res_08	4-(3,5-dimethoxyphenyl)-1-(3,4,5-trimethoxyphenyl)-1*H*-imidazole	> 100	44.5 ± 0.33
Res_09	5-(4-methoxyphenyl)-1-methyl-2-(3,4,5-trimethoxyphenyl)-1*H*-imidazole	> 100	45.1 ± 0.49
Res_10	4-(3,5-dimethoxyphenyl)-1-(4-methoxyphenyl)-1*H*-imidazole	> 100	39.9 ± 0.72
Res_11	2-(3,5-dimethoxyphenyl)-5-(4-methoxyphenyl)-1-methyl-1*H*-imidazole	> 100	32.6 ± 1
Res_12	2-(3,5-dimethoxyphenyl)-1-methyl-5-(3,4,5-trimethoxyphenyl)-1*H*-imidazole	54.51 ± 1.92	41.81 ± 0.50
Res_13	5-(3,5-dimethoxyphenyl)-2-(4-methoxyphenyl)-1-methyl-1*H*-imidazole	50.69 ± 2.38	42.51 ± 0.61
Res_14	2-(4-methoxyphenyl)-1-methyl-5-(3,4,5-trimethoxyphenyl)-1*H*-imidazole	> 100	44.4 ± 0.56
Res_15	1-(3,5-dimethoxyphenyl)-4-(4-methoxyphenyl)-1*H*-imidazole	52.99 ± 1.67	18.21 ± 0.87
Res_16	1-(4-methoxyphenyl)-4-(3,4,5-trimethoxyphenyl)-1*H*-imidazole	54.02 ± 3.83	43.9 ± 0.71
Res_18	1-(3,5-dimethoxyphenyl)-4-(3,4,5-trimethoxyphenyl)-1*H*-imidazole	> 100	41.33 ± 0.69
Res_19	5-(3,5-dimethoxyphenyl)-1-methyl-2-(3,4,5-trimethoxyphenyl)-1*H*-imidazole	50.77 ± 2.91	41.9 ± 0.32

[a] The IC50 values (μM) are the concentrations corresponding to 50% inhibition of cell viability. IC50 values were determined by MTT assay after 24 h and 72 h of incubation.

Table 2. IC50 values were calculated by performing dose-response experiments with resveratrol and analogues in ascites derived tumor cells.

	OvCa1		OvCa2		OvCa3	
Compound	**IC_{50}[a] 24h (μM)**	**IC_{50} 72h (μM)**	**IC_{50}[a] 24h (μM)**	**IC_{50} 72h (μM)**	**IC_{50}[a] 24h (μM)**	**IC_{50} 72h (μM)**
Res	> 100	40.45 ± 0.42	> 100	41.25 ± 1.25	> 100	38 ± 2.02
Res_04	35.12 ± 1.20	18.50 ± 0.34	34.20 ± 1	20.10 ± 1.56	35.68 ± 0.56	20.55 ± 0.60
Res_08	> 100	34.42 ± 0.78	> 100	33.50 ± 0.56	> 100	32.10 ± 1.60
Res_09	> 100	38.2 ± 0.58	> 100	36.30 ± 1.10	> 100	35.70 ± 0.10
Res_10	> 100	35.43 ± 0.42	> 100	34.40 ± 0.65	> 100	35.21 ± 1
Res_11	> 100	28.2 ± 2.31	> 100	27 ± 0.40	> 100	25.76 ± 2.37
Res_12	43.21 ± 1.92	38 ± 0.76	44.50 ± 2.20	38.42 ± 0.52	44.12 ± 1.10	39.70 ± 1.02
Res_13	42.01 ± 1.22	37.31 ± 0.11	43 ± 1.45	36.55 ± 0.35	42.77 ± 0.50	36.44 ± 0.59
Res_14	> 100	36.20 ± 1.60	> 100	35.10 ± 0.95	> 100	35.20 ± 0.47
Res_15	34.31 ± 0.95	12.41 ± 1.25	35.27 ± 1.05	14.52 ± 1.45	36.59 ± 0.35	16.12 ± 0.30
Res_16	39.34 ± 2.23	36.2 ± 1.23	38.24 ± 1.90	35.33 ± 2.03	35 ± 2.08	35.78 ± 1.75
Res_18	> 100	31.35 ± 1.90	> 100	31 ± 0.90	> 100	32.05 ± 1.04
Res_19	45.67 ± 2.56	35.60 ± 0.25	44.42 ± 2.40	34.76 ± 1.29	43.23 ± 1.66	33.39 ± 0.91

[a] The IC50 values (μM) are the concentrations corresponding to 50% inhibition of cell viability. IC50 values were determined by MTT assay after 24 h and 72 h of incubation.

Table 3. IC50 values for each combination were calculated by performing dose-response experiments in ascites derived tumor cells.

	OvCA1		OvCA2		OvCA3	
Treatment group	**IC50 (nM)**	**P value**	**IC50 (nM)**	**P value**	**IC50 (nM)**	**P value**
Paclitaxel	6.3 ± 1.1	/	4.4 ± 2	/	5.2 ± 0.9	/
Paclitaxel / EGF	10.5 ± 1.5	***	8.7 ± 0.8	***	7.3 ± 1.1	***
Paclitaxel / EGF / Res	7.4 ± 0.6	/	5.8 ± 1.5	/	6.1 ± 0.5	/
Paclitaxel / EGF / Res_15	6.1 ± 1.2	***	4.2 ± 1	***	4.8 ± 0.4	***
Paclitaxel / IL-6	9.1 ± 1.4	***	8.1 ± 0.2	***	7.9 ± 0.7	***
Paclitaxel / IL-6 / Res	7.1 ± 2	/	5.2 ± 0.1	/	6.2 ± 1.1	/
Paclitaxel / IL-6 / Res_15	6.4 ± 0.5	***	4.1 ± 0.2	***	5.5 ± 0.4	***

Ascitic cells were treated with paclitaxel alone, paclitaxel plus resveratrol (40 μM), paclitaxel plus Res_15 (10 μM), plus EGF (100 ng mL^{-1}), and IL-6 (10 ng mL^{-1}) for 72 h. Cell viability was assayed using MTT. Data represent mean values ± S.D from three independent experiments. *P values, compared with paclitaxel alone.

Supplementary Table 1. List of antibodies used in western blotting.

Antibody name	Company	Dilution
Anti-Akt	Santa Cruz Biotechnology (sc-5298)	1:1000
Anti-Cofilin	Santa Cruz Biotechnology (sc-33779)	1:1000
Anti-phospho Cofilin (ser3)	Santa Cruz Biotechnology (sc-21867-R)	1:1000
Anti-Cyclin D1	Santa Cruz Biotechnology (sc-20044)	1:200
Anti-E-cadherin	Santa Cruz Biotechnology (sc-71009)	1:1000
Anti-phospho-GSK3β	Santa Cruz Biotechnology (sc-11757)	1:500
Anti-N-cadherin	Santa Cruz Biotechnology (sc-59987)	1:1000
Anti-Slug	Santa Cruz Biotechnology (sc-166902)	1:500
Anti-Vimentin	Santa Cruz Biotechnology (sc-7558)	1:500
Anti-Zeb1	Santa Cruz Biotechnology (sc-25388)	1:500
Anti-α Tubulin	Santa Cruz Biotechnology (sc-23948)	1:2000
Anti-β Catenin	Santa Cruz Biotechnology (sc-1496)	1:1000
Anti-Bcl2	Cell Signaling (D55G8)	1:1000
Anti-GSK3β	Cell Signaling (D5C5Z)	1:1000
Anti-pospho-Akt (ser473)	Cell Signaling (4051)	1:1000
Anti-phospho-p44/42 MAPK (Erk 1/2)	Cell Signaling (4695)	1:2000
Anti-phospho-p44/42 MAPK (Erk 1/2) (thr202/tyr204)	Cell Signaling (4370)	1:2000
Anti-phospho-GSK3 (tyr279/tyr216)	Millipore (05-413)	1:500

Supplementary Table 2. Oligonucleotides used for Real time PCR analysis.

Gene	Accession number (NCBI)	Primer 5′-3′	bp
CDH2	NM_001792.4	N-cad F: CAGGAAAAGTGGCAAGTGGC N-cad R: AGGAAAAGGTCCCCTGGAG	197
VIM	NM_003380.3	VIM F: TGGCCGACGCCATCAACACC VIM R: CACCTCGACGCGGGCTTTGT	227
ZEB1	NM_001174096.1	ZEB1 F: GGCCCCAGGTGTAAGCGCAG ZEB1 R: CTGTTGGCAGGTCATCCTC	181
ZEB2	NM_014795.3	ZEB2 F: AAGCCAGGGACAGATCAGC ZEB2 R: GCAGTTTGGGCACTCGTAAG	156
SLUG	NM_003068.4	Slug F: CAACGCCTCCAAAAAGCCAA Slug R: ACTCACTCGCCCCAAAGATG	229
NRF1	NM_005011.3	NRF F: CCGTTGCCCAAGTGAATTAT NRF R: ACTGTAGCTCCCTGCTGCAT	181
PPARGC1A	NM_013261.3	PGC1aF: GCTGACAGATGGAGACGTGA PGC1aR: TGCATGGTTCTGGGTACTGA	178
SIRT1	NM_001142498.1	sirt F: TGTTGGTTCTAGTACTGGGG sirt R: CCTCAGCGCCATGGAAAATG	164
TFAM	NM_001270782.1	Tfam F: CCGAGGTGGTTTTCATCTGT Tfam R: ACGCTGGGCAATTCTTCTAA	147
Rplp0	NM_001697.2	36B4 F: TCGACAATGGCAGCATCTAC 36B4 R: ATCCGTCTCCACAGACAAGG	191

Supplementary Figure Legends

Supplementary Figure 1. Chemical structures of resveratrol analogues. They belong to two distinct classes of bis-arylated imidazoles: 1,5-diaryl substituted imidazoles (Res_04, Res_08, Res_10, Res_15, Res_18), and 2,5-diaryl substituted 1-methylimidazoles (Res_09, Res_11, Res_12, Res_13, Res_14, Res_19).

Supplementary Figure 2. Resveratrol analogues effects on NHDF cell proliferation. Cells were treated with resveratrol or analogues at 25 μM for 72 h. Data shown represent the mean ± SD of three independent experiments and values were taken from at least six wells from each experiment.

Supplementary Figure 3. Densitometric analysis of western blotting data. Results (mean ± SD; n = 3) are expressed as fold change of CTR values, and represent the ratio between N-cadherin, Cyclin D1, β-catenin, Bcl2, and α-tubulin levels. pCof, pErk, pGsk, and pAkt were normalised over total Cof, Erk, Gsk, Akt. Data were analyzed by Student's t-test. * $p<0.05$; ** $p<0.01$; *** $p<0.001$ as compared with resveratrol treated cells.

Supplementary Figure 4. qPCR analysis on the expression of resveratrol targets in SKOV-3 cells treated for 24 h with Res and Res_15 at the concentration of 100 uM and 25 uM, respectively. Data are represented as mean ± SD of three independent experiments. The only asterisks indicate a significant difference compared to control, whereas asterisks above a line represent a significant difference between resveratrol and Res_15 treated samples. One-way ANOVA analysis * $p<0.05$; ** $p<0.01$; *** $p<0.001$.

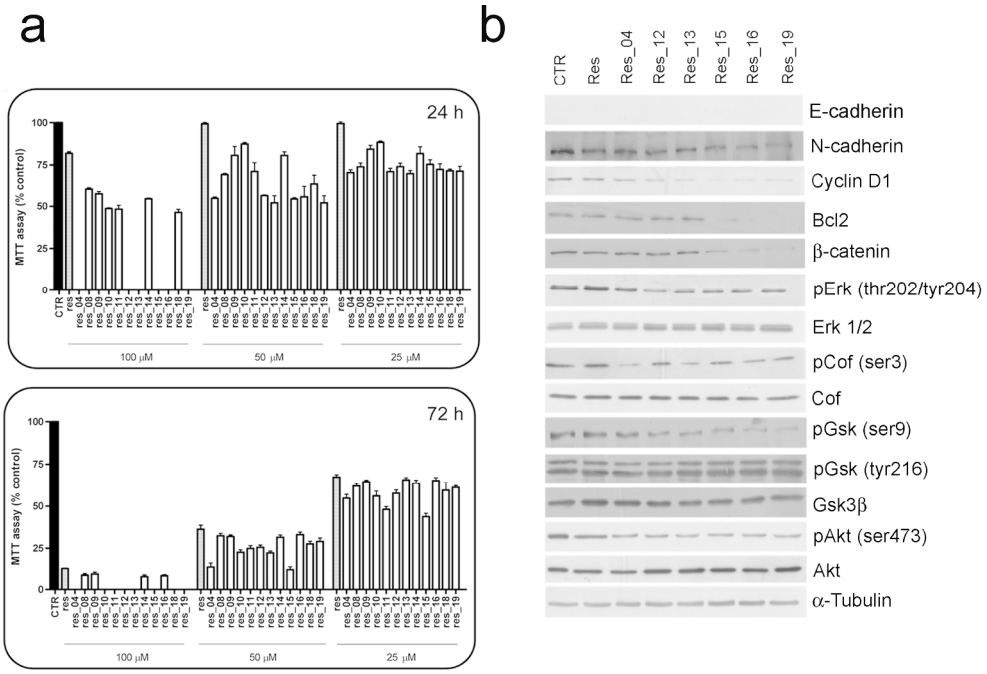
a
b
24 h
72 h
MTT assay (% control)
100 μM
50 μM
25 μM
CTR
Res
Res_04
Res_12
Res_13
Res_15
Res_16
Res_19
E-cadherin
N-cadherin
Cyclin D1
Bcl2
β-catenin
pErk (thr202/tyr204)
Erk 1/2
pCof (ser3)
Cof
pGsk (ser9)
pGsk (tyr216)
Gsk3β
pAkt (ser473)
Akt
α-Tubulin

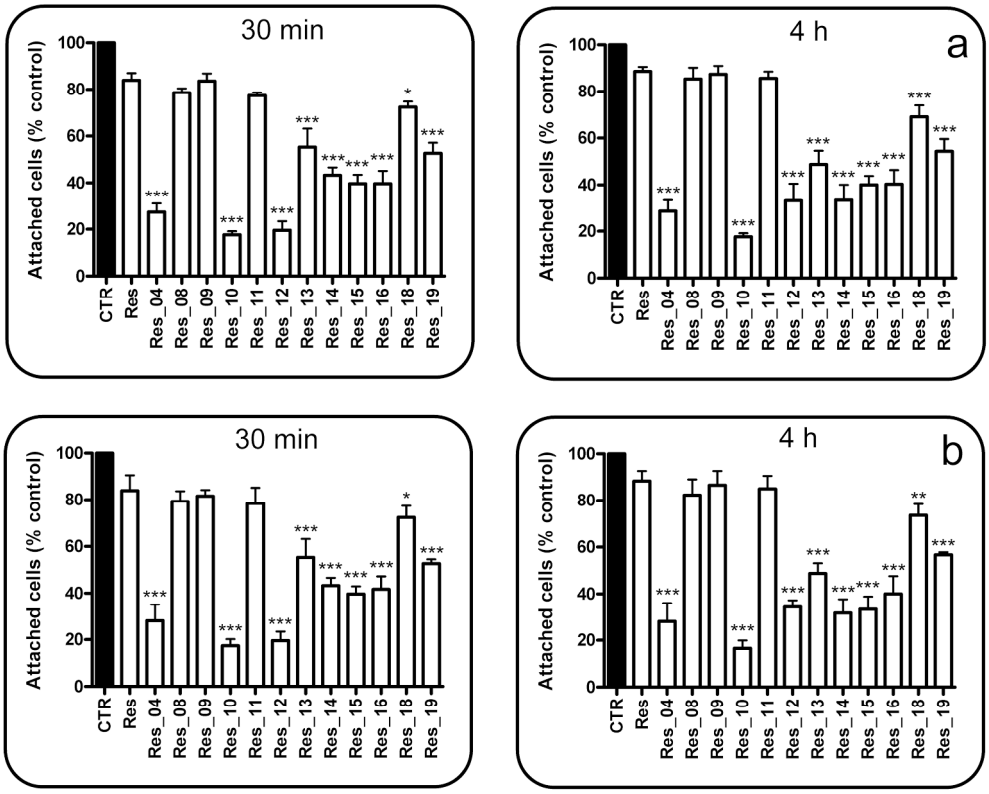
30 min
4 h
a
30 min
4 h
b
Attached cells (% control)
CTR
Res
Res_04
Res_08
Res_09
Res_10
Res_11
Res_12
Res_13
Res_14
Res_15
Res_16
Res_18
Res_19

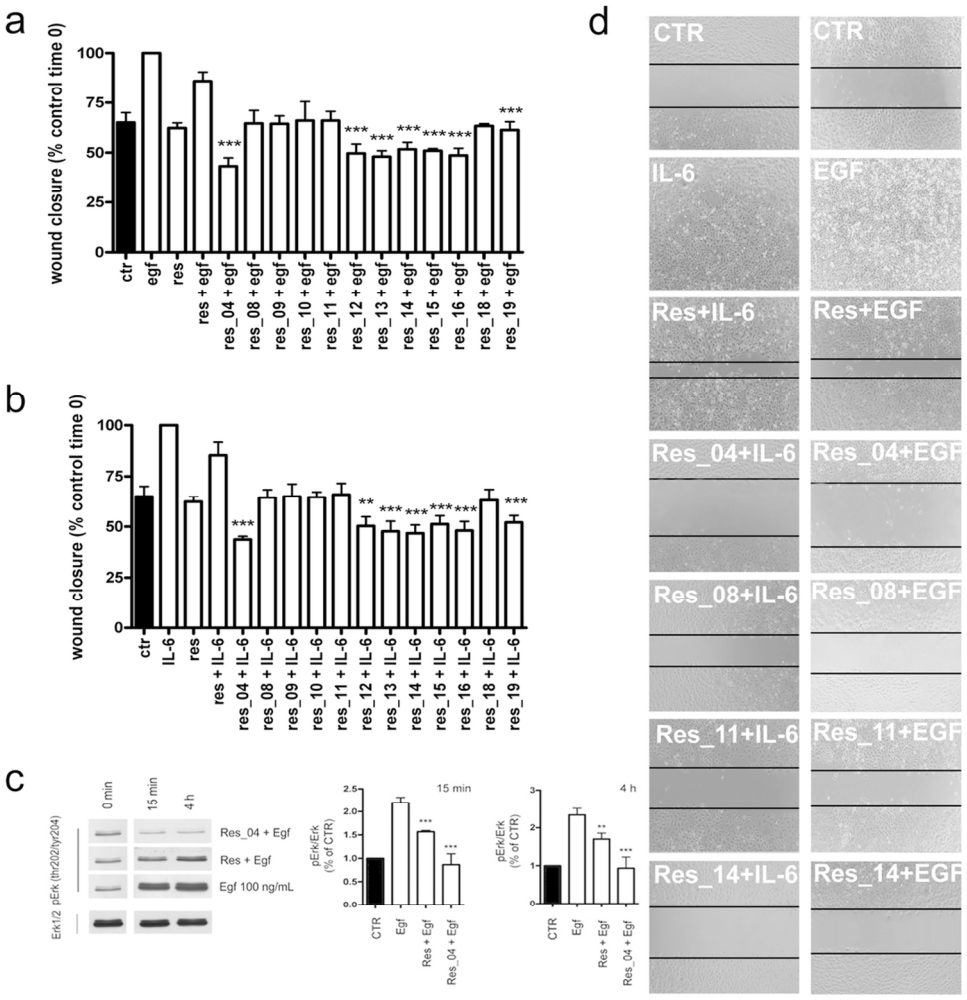

101x103mm (300 x 300 DPI)

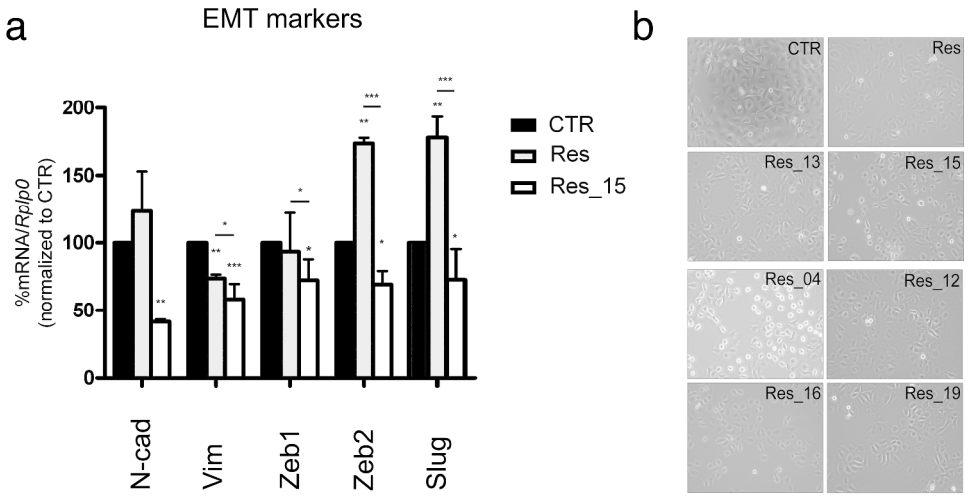
a
EMT markers
%mRNA/Rplp0
(normalized to CTR)
200
150
100
50
0
CTR
Res
Res_15
N-cad
Vim
Zeb1
Zeb2
Slug
b
CTR
Res
Res_13
Res_15
Res_04
Res_12
Res_16
Res_19

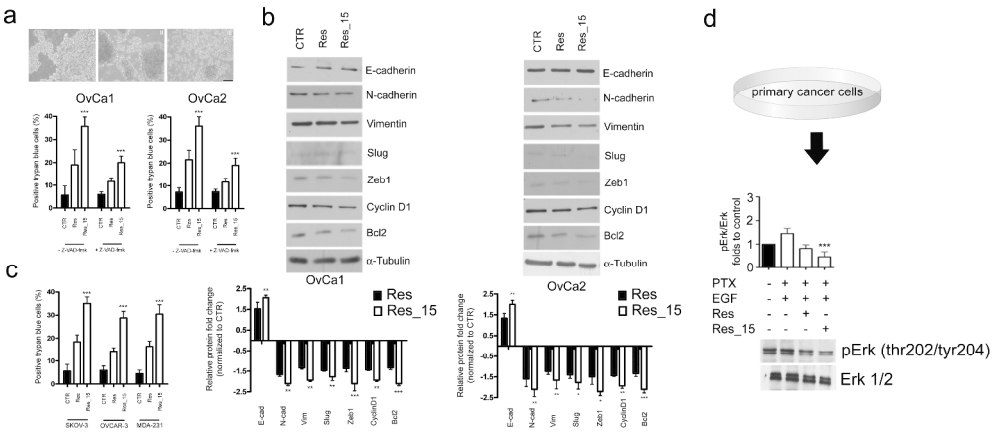
a
OvCa1
OvCa2
Positive trypan blue cells (%)
- Z-VAD-fmk
+ Z-VAD-fmk
b
CTR
Res
Res_15
E-cadherin
N-cadherin
Vimentin
Slug
Zeb1
Cyclin D1
Bcl2
α-Tubulin
OvCa1
OvCa2
c
SKOV-3
OVCAR-3
MDA-231
Relative protein fold change (normalized to CTR)
Res
Res_15
E-cad
N-cad
Vim
Slug
Zeb1
CyclinD1
Bcl2
d
primary cancer cells
pErk/Erk folds to control
PTX
EGF
Res
Res_15
pErk (thr202/tyr204)
Erk 1/2

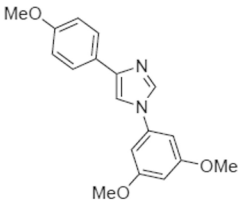

RES_15

$C_{18}H_{18}N_2O_3$
Mol. Wt.: 310,35

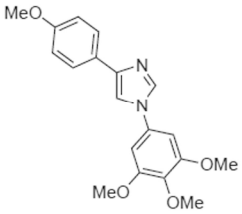

RES_04

$C_{19}H_{20}N_2O_4$
Mol. Wt.: 340,37

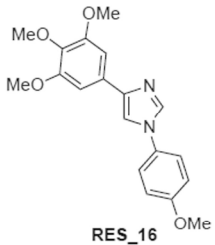

RES_16

$C_{19}H_{20}N_2O_4$
Mol. Wt.: 340,37

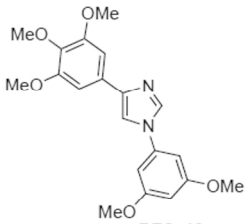

RES_18

$C_{20}H_{22}N_2O_5$
Mol. Wt.: 370,40

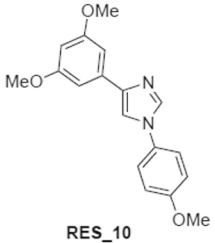

RES_10

$C_{18}H_{18}N_2O_3$
Mol. Wt.: 310,35

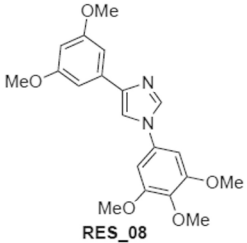

RES_08

$C_{20}H_{22}N_2O_5$
Mol. Wt.: 370,40

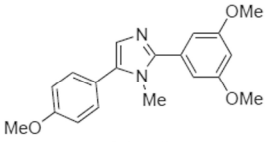

RES_11

$C_{19}H_{20}N_2O_3$
Mol. Wt.: 324,37

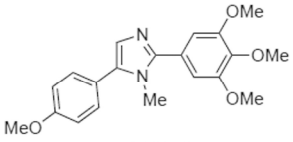

RES_09

$C_{20}H_{22}N_2O_4$
Mol. Wt.: 354,40

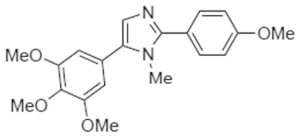

RES_14

$C_{20}H_{22}N_2O_4$
Mol. Wt.: 354,40

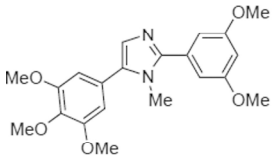

RES_12

$C_{21}H_{24}N_2O_5$
Mol. Wt.: 384,43

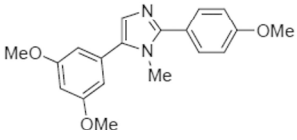

RES_13

$C_{19}H_{20}N_2O_3$
Mol. Wt.: 324,37

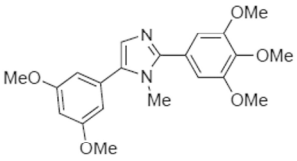

RES_19

$C_{21}H_{24}N_2O_5$
Mol. Wt.: 384,43

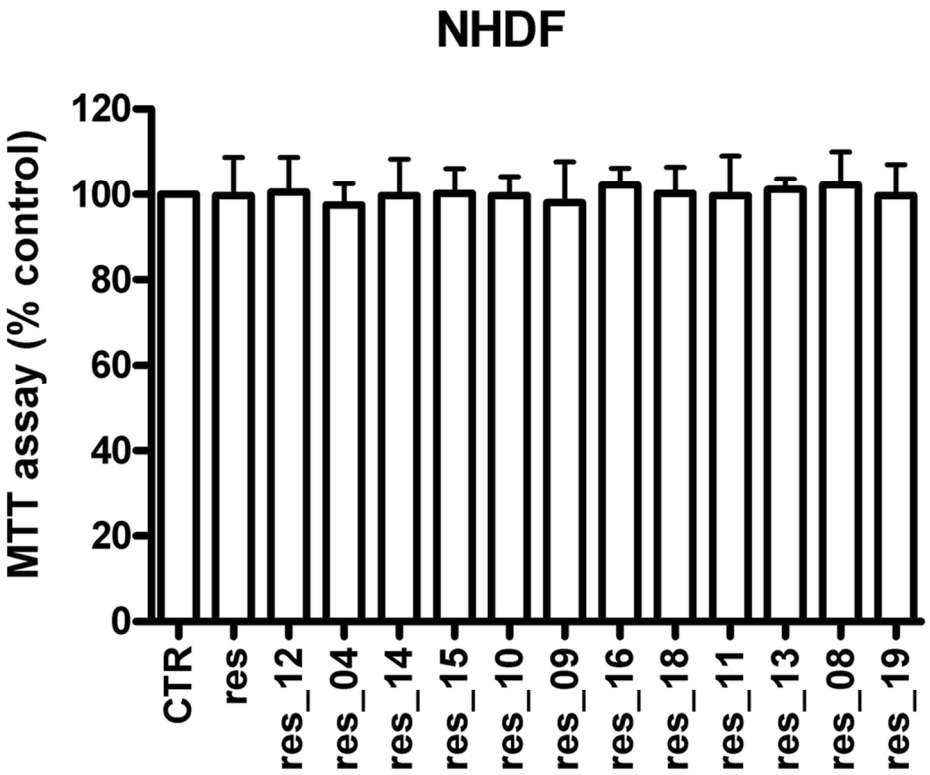

94x76mm (300 x 300 DPI)

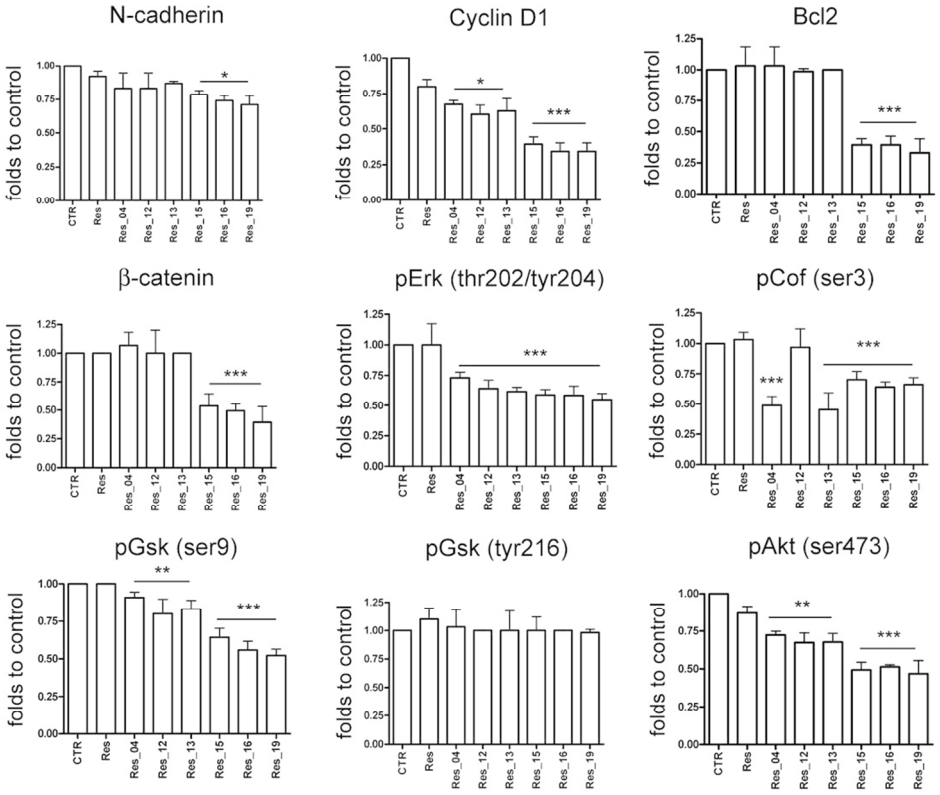

99x82mm (300 x 300 DPI)

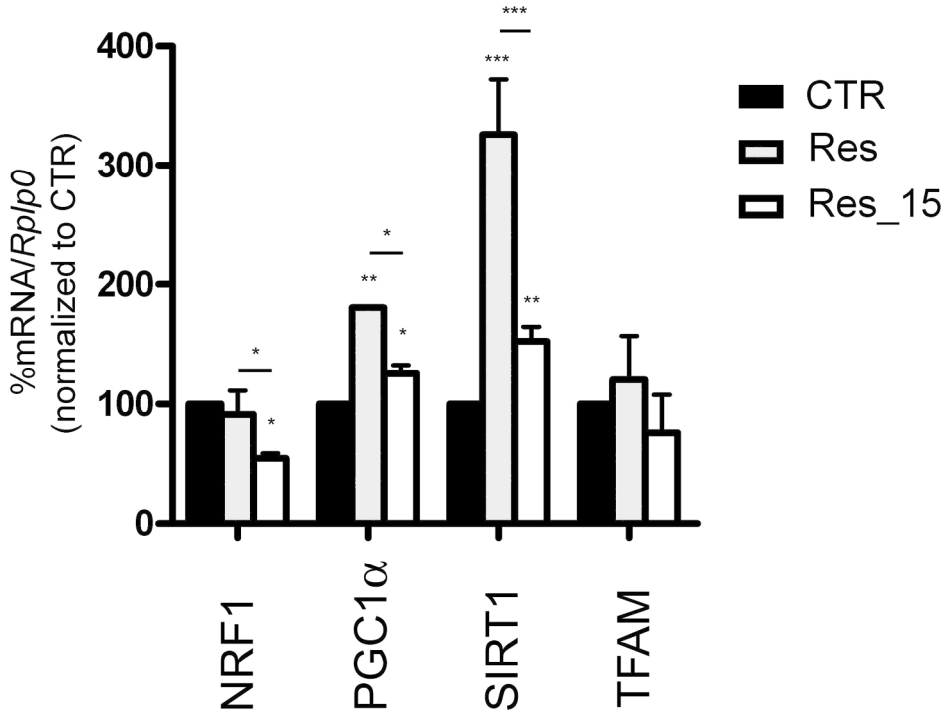
Resveratrol targets
%mRNA/Rplp0
(normalized to CTR)
400
300
200
100
0
CTR
Res
Res_15
NRF1
PGC1α
SIRT1
TFAM
*
**
***